ISSN 0006-3509, Biophysics, 2020, Vol. 65, No. 2, pp. 250–258. © Pleiades Publishing, Inc., 2020.
Russian Text © The Author(s), 2020, published in Biofizika, 2020, Vol. 65, No. 2, pp. 290–299.

CELL BIOPHYSICS

Cytoplasmic Streaming as an Intracellular Conveyer: Effect on Photosynthesis and H^+ Fluxes in *Chara* Cells

A. A. Bulychev[a], *, A. V. Alova[a], N. A. Krupenina[a], and A. B. Rubin[a]

[a]*Department of Biology, Moscow State University, Moscow, 119991 Russia*

**e-mail: bulychev@biophys.msu.ru*

Received November 8, 2019; revised November 30, 2019; accepted January 21, 2020

Abstract—Giant-sized cells, such as the internodes of characean algae, demonstrate rapid (up to 100 μm/s) rotational cytoplasmic streaming that participates in long-distance intracellular interactions and coordinates the functional activity of organelles under a nonuniform light environment. The specific functions of intense cytoplasmic streaming remain poorly investigated. The lateral transport of photometabolites can be detected by combining pinhole illumination with measurements of chlorophyll fluorescence and external pH on microscopic cell regions located downstream of the locally illuminated area. The involvement of cyclosis in regulation of photosynthesis and plasmalemmal H^+ transport was revealed by this means. In regions exposed to bright local light, the chloroplasts export reducing equivalents and triose phosphates into the streaming cytoplasm that spread over the cell and induce a transient rise of chlorophyll fluorescence in shaded cell areas located far from the site of photostimulus application. This review highlights the properties of cyclosis-mediated fluorescence changes, including the photoinduction of long-distance transmission, sensitivity to metabolic inhibitors, its nonuniform spatial distribution in illuminated cells, and gradual (1–5 min) inactivation of long-range signaling after transferring the cell to darkness. A stimulatory influence of the action potential on long-distance signal transmission is shown. The new method is suitable for studying the intercellular transport of metabolites and the permeability of plasmodesmata.

Keywords: cytoplasmic streaming, long-range signaling, nonuniform pH profiles, remote regulation of photosystem II activity, plasmodesmata

DOI: 10.1134/S0006350920020037

The term "intracellular conveyer" is not often found in publications on cell biophysics and biochemistry. The idea of a conveyer reminds one of a continuously moving production belt with incoming workpieces that are processed as they move from the starting position to the destination site. In plant cells, a similar role is played by the cytoplasmic streaming. The mobility of the cytoplasm has been known for almost 250 years: it was first described in 1774 by the Italian physicist Bonaventura Corti who observed *Chara* alga cells under a microscope. Over the past half century, a great advance has been achieved in understanding the mechanism of cytoplasmic movement [1, 2]. Significantly less is known about the functional role of intracellular fluid flows. Based on general concepts, the proposed function of cytoplasmic flow consists in smoothing the intracellular concentration gradients [3, 4]. The stream distributes substances throughout the cell and delivers them to intercellular barriers, which facilitates the transfer of signaling substances and assimilates over long distances towards the zones of active growth. Specific examples of the implications of fluid flow in cellular processes remain scarce.

Long-distance transport is one of the most important processes in plants; it always includes the intracellular and transcellular stages that correspond to the distribution of a substance within the cytoplasm and its passage through intercellular contacts, that is, plasmodesmata [4]. The cell–to–cell transport of substances was often studied by microinjecting fluorescent dyes, such as carboxyfluorescein [5, 6]. However, this invasive method does not ensure precise localization of the injected probe in the cytoplasm or vacuole; it also disturbs the cellular composition and internal hydrostatic pressure within the cell, which hampers clear interpretation of the results. Therefore, the search for non-damaging methods and adequate model objects becomes highly important. Characean algae are the closest phylogenetic relatives of higher plants [7] and represent one of the most convenient plant cell models.

The thallus of *Chara* alga consists of alternating giant internodal cells and small nodal cells. The large sizes of the internodes determine the occurrence of

Abbreviations: Q_A, primary quinone acceptor of photosystem II, PSII, photosystem II, PSI, photosystem I.

special and even unique properties. These cells are electrically excitable: the voltage-gated and Ca^{2+}-gated ion channels of the plasmalemma and tonoplast were first identified with characean species [8, 9]. *Chara* cells are capable of self-organization, which is evident in light-dependent formation of heterogeneous longitudinal profiles of surface pH and photosynthesis [10–15]. They exhibit an exceptionally rapid, up to 100 μm/s, cytoplasmic streaming [16, 17]. *Chara* cells demonstrate biogenic calcification, i.e., metabolically related precipitation of calcium crystals on cell walls at high pH zones [18]. These cells are capable of healing small wounds to escape large losses in biomass upon the death of individual cells [19, 20]. Cell chains are convenient for studying communications between neighbor cells. The internodal cells are well suited for microfluorometric assays of chlorophyll fluorescence, since chloroplasts are immobile and packed in a single layer over the cell periphery.

The giant (up to 10 cm) cell dimensions of *Chara corallina* and *C. australis* (up to 20 cm in *Nitellopsis*) dictate the need for specific mechanisms of signal transmission. In small cells, reagents mix for less than 1 s, but diffusion over a distance of 5 cm would take several weeks. Obviously, characean algae employ other means for regulation and coordination of cell processes.

Rapid signal transmission can be achieved through propagation of electrical pulses, that is, action potentials [21]. Action potentials move along the cell at the velocity of ~1 cm/s. Hence, this short (~2 s) depolarization wave that is associated with an almost 100-fold increase in cytoplasmic Ca^{2+} level propagates over the cell length in less than 10 s. However, action potentials arise only in adverse conditions (mechanical impact or leakage of electrolytes from damaged cells) but are usually absent in cells at rest. Under physiological conditions, the signal and metabolite transmission is mainly mediated by cytoplasmic streaming. Assuming the streaming layer thickness of ~5 μm and the cell diameter of 0.7 mm, the fluid volume passing across the cytoplasm cross section is ~1 nL/s. Chloroplasts are densely packed in rows along the cell periphery and are located at the boundary between the streaming endoplasm and stagnant ectoplasm. On the inner side of the chloroplast layer, actin filaments are attached and serve as the rails for ATP-dependent movement of myosin molecules carrying vesicles as a cargo [20]. The vesicles entrain the adjacent water layers, thus creating rotational fluid flow. The highest speed of fluid movement is achieved at the boundary between immobile chloroplasts and the flowing endoplasm [3, 22]. The fluid movement along the closed trajectory is termed rotational streaming. Counter-directed flows are separated by a transparent neutral line. Within this line, the cytoplasmic layer is narrow and leaves no space for plastids. The fluid flow is directed along a slightly twisted spiral path. The flow rate strongly depends on temperature and to a lesser extent on other physical factors. The action potential causes a temporary (for 30 s) cessation of movement and a slow (5–10 min) recovery of the flow rate to the initial level.

The distribution of substances over the cell with a fluid flow is obviously significant when the cytoplasmic composition is spatially heterogeneous. Such a situation arises, for example, under uneven illumination, when bright light hits a cell part, while other parts remain in the shade. The transfer of excess products of light reactions from a saturating light area to shaded chloroplasts, whose CO_2-fixation capacity is underloaded due to the lack of these products, can improve net photosynthesis. The effective intracellular distribution of photometabolites requires not only a rapid cytoplasmic flow but also the rapid exchange between chloroplasts and the cytoplasm. The major transport systems of the plastid envelope are the so-called "malate valve" and the triose phosphate translocator [23, 24]. Both systems operate as redox shuttles: they remove NAD(P)H from illuminated chloroplasts, since NADPH is formed in excess in comparison with ATP during linear photosynthetic electron flow. Both carriers are light dependent and lose their activity in the dark [24].

The influence of cytoplasmic streaming on cellular processes can be studied by applying a narrow light beam (0.4 mm in diameter) to the cell via an optic fiber and observing consequent changes in chlorophyll fluorescence and cell surface pH at a distance of 1–6 mm from the site of local illumination [25, 26]. Chlorophyll fluorescence is excited by weak modulated light (Pulse Modulated Fluorometry, PAM) that does not affect the chloroplast condition. In addition, the entire cell is exposed to weak background light (~10 μmol m^{-2} s^{-1}), which keeps the photosynthetic apparatus in an active state. Measurements of pH in unstirred layers of the external medium provide information on direction and magnitude of H^+ fluxes across the plasma membrane domains.

Under local illumination, the metabolites are exported from the chloroplast stroma to the cytoplasm that streams with the highest velocity at the border to the stationary layer of chloroplasts. The exported metabolites move laterally in the form of a packet, whose size is determined by the duration of illumination and the cytoplasmic flow rate. The time traveled by the package until its arrival to the analyzed region determines the lag phase duration of the fluorescence and pH responses. When the metabolites reach the analyzed area, they cause transient changes in both parameters. These changes reflect the cyclosis-mediated remote regulatory action of light on chloroplasts and the plasma membrane [27].

The first results obtained under spatial separation of photostimulation area and the region accommodating functional changes were presented in a few experimental and review articles [28–33]. In the present

work, we focus on later studies not considered in reviews [31, 32].

Measurements of cell surface pH in slightly alkaline cell regions revealed that local illumination of neighbor regions located upstream in the cytoplasmic flow produces in 3–4 min a strongly alkaline zone, with a pH shift of up to 2 units between the initial and final values. When the light beam was applied at the same distance from the analyzed area on the downstream side, no alkaline zone was formed. These results indicate that in the light chloroplasts release a product that is transported with the cytoplasmic flow and induces the formation of an external alkaline zone [34]. Thus, the generation of inhomogeneous pH profiles in internodal cells during illumination is closely related to the movement of metabolites in the cytoplasmic stream.

In similar experiments with short (30 s) local light exposures, the pH shifts were measured separately in alkaline and acidic zones. Local illumination of a cell part located upstream in the cytoplasmic flow from the analyzed region caused the pH to increase in the alkaline zone by ~0.05 units and to decrease in the acidic zone. The time $t_{1/2}$ from the onset of a local light pulse to half of the pH shift depended linearly on the distance d between the light source and the measurement site. The linear plots of $t_{1/2}$ as a function of distance d for the alkaline and acidic zones had equal slopes (angular coefficient 17.4 ± 2 s/mm); however, the time $t_{1/2}$ for the acidic zone was approximately 15 s shorter than for the alkaline zone, and this difference remained unaltered upon variations of distance d from 1 to 3 mm. Apparently, there are two different intermediates, one of which enters the cytoplasm earlier than the other. The "fast" intermediate is primarily responsible for the activation of the plasmalemmal H^+ pump, while the "delayed" agent accounts for the increase in passive H^+ conductance of the plasma membrane. Judging by equal slopes of the linear plots for $t_{1/2}$ on the distance d, both intermediates move in the cytoplasmic flow at equal velocities of ~60 μm/s.

Metabolites exported by chloroplasts in the light affect not only the plasmalemma but also the chloroplasts located downstream of the illuminated zone. This is manifested in a transient increase in chlorophyll fluorescence by approximately 25% after a latent period of 20 to 30 s [35]. An increase in fluorescence signifies that metabolites exported by illuminated chloroplasts reached the shaded areas, entered the plastid stroma, and transiently reduced the plastoquinone pool, including the primary quinone acceptor Q_A, which is known to control the emission of photosystem II (PSII). The position of the fluorescence peak nearly coincides with the interval of development of the pH shift. However, the plots of F' peak position as a function of distance to the light source overlapped for the alkaline and acid zones, unlike the shift between respective graphs for the pH changes. It should be noted that at increased intensities of background light, local illumination induced fluorescence quenching that succeeded the initial fluorescence rise [25].

An actin polymerization inhibitor, cytochalasin D, that completely arrests cytoplasmic streaming [36] helped to prove that microfluidic transmission of a fluorescence-controlling signal occurs. The cessation of streaming was accompanied by elimination of fluorescence changes in response to local illumination of a remote cell part [37, 38], whereas washing the cell with a fresh medium and the resumption of streaming restored the responses to local photostimuli. At intermediate flow rates, the fluorescence peak was delayed for tens of seconds, and it became wider and smaller in amplitude. The broadening of the peak was ascribed to diffusion. The longer travel of the metabolite package until its delivery to the analyzed area allows more time for diffusion to alter the package width and the shape of F' changes in response to local illumination. With account for translational movement of the metabolites in the package, their diffusion during transport, and the partial consumption of metabolites along their lateral transfer, qualitative agreement was obtained between the experimental kinetics of F' changes and the F' curves simulated with a mathematical model [27]. The model described the dynamics of F' changes both under uniform translational movement of the cytoplasm and under variable flow rates when cyclosis underwent recovery after its temporary stoppage at the moment of generation of an action potential.

Similar modifications of the F' fluorescence signal also occur at a constant flow rate if the distance between the local light source and the measurement region is increased [38]. At short separating distances (1–1.5 mm), the F' peak is attained rather rapidly and has a large amplitude. At large distances (d = 3–4.5 mm), the peak develops after a long delay, and the bandwidth of the F' changes becomes wider. The dependence of the position of F' on distance can be illustrated by the diagram in Fig. 1. The larger the distance is between the optic fiber and the measurement area, the longer the time is that passes from the onset of local illumination until the peak of fluorescence is reached. Drawing a straight line along F' peaks in this diagram is a method to estimate the travel velocity for the metabolite that causes distant changes in fluorescence. In the given case, the increase in the path length by 3.5 mm shifted the F' peak position by 65 s. Thus, the propagation rate of the regulatory factor was 54 μm/s. This velocity is approximately one-third lower than the speed of particle movement measured under a microscope in transmitted light. An appreciable deceleration of the transmission is possibly due to the fact that the moving metabolite binds repeatedly and reversibly to stationary intracellular structures [39].

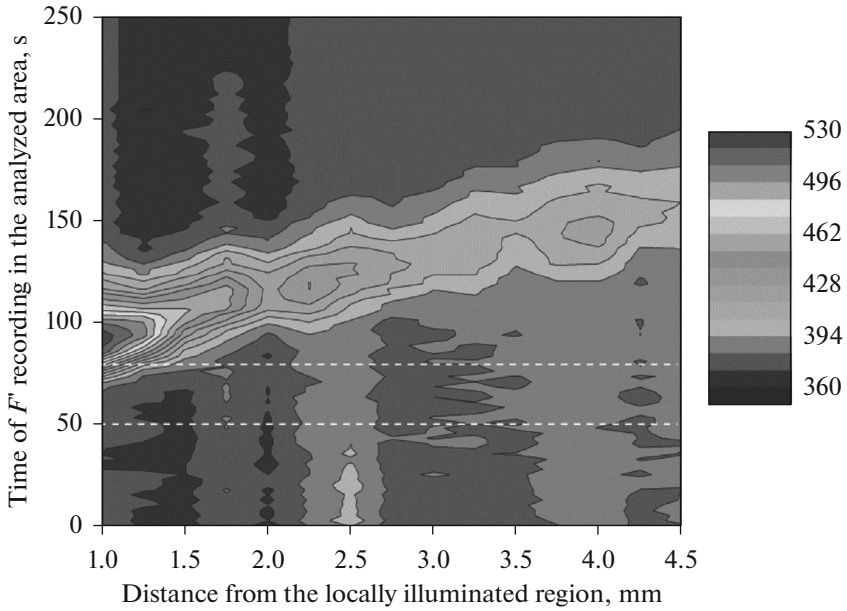

Fig. 1. A diagram of *F'* chlorophyll fluorescence changes at various distances from the area of local illumination to the analyzed zone. The cytoplasmic flow is directed from the position of optic fiber to the fluorometric area. Black and white gradations correspond to different fluorescence intensities. The horizontal dashed lines mark the moments when local illumination was turned on and off (at $t = 50$ and 80 s from the start of *F'* recording, respectively).

The principal stages of distant transmission of the metabolic signal have different locations and functions: (1) the formation and export of photometabolites in a brightly lit cell area, (2) the downstream transfer of exported substrates with a cytoplasmic flow up to 5–6 mm, (3) the import of triose phosphates and reducing equivalents from the fluid stream to the stroma of shaded chloroplasts, and (4) biochemical and redox reactions that cause the reduction of plastoquinone and the PSII quinone acceptor, with the consequent fluorescence rise to the peak. After the metabolite passed by the measurement area, the indicator of the chloroplast condition, *F'* returns to its normal level, sometimes with non-monotonic kinetics. Fluorescence drops for 2–3 min slightly below the initial level, while the quantum yield of PSII photoreaction increases. A possible reason for the *F'* undershoot is the enhanced electron efflux from the plastoquinone pool due to reductive activation of CO_2-assimilating enzymes and a respective increase in NADPH consumption [39].

Deciphering the role and features of individual steps in microfluidic signaling should depend on selective treatments. As an example, cytochalasin D known to influence actin filaments selectively suppressed the stage of metabolite lateral transport. Unfortunately, in many cases it is impossible to separate the action of inhibitors at the initial and final stages of the signaling pathway. Specifically, signal transmission was irreversibly suppressed by diphenyleneiodonium and methyl viologen [35]. Both reagents are known to disturb electron transfer in the region beyond photosystem I (PSI). Diphenyleneiodonium inhibits ferredoxin-NADP reductase and flavin enzymes. Methyl viologen switches the CO_2-dependent photosynthetic electron flux to the O_2 reduction pathway. In resting *Chara* cells, this herbicide has no access to its targets even after a long (30 min) incubation. However, its impact develops instantly after a single generation of the action potential [15, 40]. Apparently, methyl viologen, as a divalent cation, permeates into the cell through Ca^{2+}-permeable voltage-gated channels that are also permeable to other divalent cations. The results of experiments with inhibitors emphasize the role of reactions that occur on the acceptor side of PSI and in the chloroplast stroma. However, it remains uncertain whether diphenyleneiodonium and methyl viologen disrupt the formation and export of metabolites (stage 1) or if they interfere with the terminal steps of the signaling chain (stages 3, 4).

It is known that the metabolite exchange between the chloroplast stroma and cytosol is light dependent [41]. Experiments involving dark inactivation and photoactivation of enzymes revealed a strong dependence of long-range signal transmission on light conditions [26, 35]. Figure 2 shows transient changes in *F'* fluorescence in response to local illumination when the entire cell was exposed to dim background light and when the background light was turned off synchronously with the onset of a local light pulse. The enzyme inactivation proceeds at the time scale of minutes. Therefore, switching off the background light at the moment of applying the remote light pulse elimi-

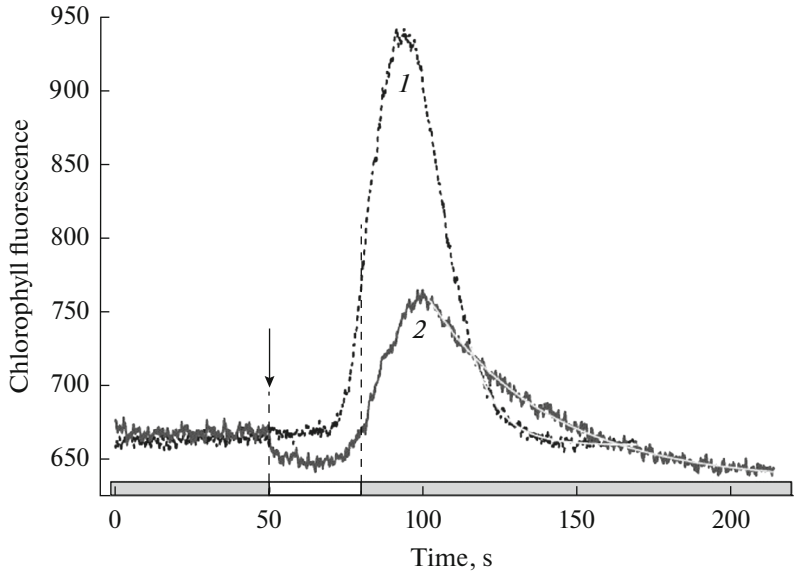

Fig. 2. Cyclosis-mediated responses of *F*' fluorescence to local illumination of a cell region located away from the place of *F*' recording under conditions when the whole cell was exposed to background illumination (14 μmol quanta m^{-2} s^{-1}, curve *1*) and when the background illumination was turned off simultaneously with application of a local light pulse (curve *2*). The arrow refers only to record 2 and marks the moment when the background light was turned off. Curves (*1*) and (*2*) are the averaged records obtained with five cells.

nates light reactions in the observation area, but does not disrupt the enzymatic processes. After placing the cell in darkness, the amplitude of fluorescence changes decreases by 2–3 times, and the signal relaxation slows. The decelerated decline of the transient *F*' fluorescence peak in darkened cells is obviously due to the cessation of chloroplast photochemical activity in the observation area. In the light, PSI oxidizes the plastoquinone pool, thus ensuring a relatively rapid decrease in *F*' after the peak, but in the dark PSI is inactive and does not participate in the oxidation of plastoquinone/Q_A. In this case, the oxidation of plastoquinone/Q_A is mediated by alternative means, e.g., plastid terminal oxidase.

It is not yet entirely clear why the *F*' response to local light is diminished when the cell is transferred to darkness. On the one hand, comparatively large *F*' responses under background light may indicate a prevalence of photochemical (PSII-dependent) plastoquinone/Q_A reduction compared to nonphotochemical reduction (dark-related electron flow from NADPH to plastoquinone) mediated by the antimycin-sensitive segment of cyclic electron transport chain [26]. However, some observations are at variance with this explanation. In some cases, *F*' responses to local beam in the absence of background illumination were larger than under background light. It is possible that the suppression of the *F*' response to local light observed after darkness results from the increased losses of the metabolite carried in the stream. In the initial dark period, the CO_2 fixation cycle and the membrane translocators remain active, while the internal NADPH resources are not replenished due to cessation of photoreactions. Further studies should clarify the extent to which the content of transported metabolites in the cytoplasm undergoes alterations upon changes in light conditions.

When the background light was switched off in advance to application of a local light pulse, the *F*' response decreased gradually with the prolongation of the dark period [26]. After 2 min of darkness, the amplitude of the *F*' response decreased by half compared to that under a zero time preceding the local light pulse; the reaction to local illumination completely disappeared after 4.5 min of dark adaptation. These changes probably reflect the inactivation of envelope translocators in the area of fluorescence measurements. The retention of transmissive condition in the dark for several minutes implies that the peak of *F*' fluorescence is related to nonphotochemical electron flux from the imported stromal reductants to the plastoquinone pool and to the reduction of Q_A quinone acceptor.

After reverse transition of dark-adapted cells to background light, the fluorescence response to local photostimulation of a remote area was initially absent; however, it was completely restored within 3 min in dim light [35]. This phenomenon of photoinduction of long-range signal transmission is similar to photoinduction of CO_2 fixation. The induction of CO_2 assimilation is known to reflect the light-dependent transition of Calvin cycle enzymes to an active state, as mediated by thioredoxin reduced by PSI. The transition of *Chara* cells to the transmissive condition

appears to include the photoactivation of translocators in the chloroplast envelope.

Microfluidic signaling has mostly been studied in low light, i.e., under conditions when the measured cell properties (fluorescence, quantum yield of PSII photoreaction, and local pH values on cell surface) were distributed uniformly along the cell length. If a pattern of alternating alkaline and acidic zones was formed under bright light, the cell capacity for long-distance regulation of PSII and chlorophyll fluorescence became also spatially nonuniform. The remote regulation of fluorescence was well expressed under acidic zones and was strongly suppressed under the alkaline zones [26, 42]. Although signal transmission was inhibited, the pH shifts in the alkaline zones remained evident in response to local illumination, indicating that the transfer of metabolites in the streaming fluid was not impaired.

One approach to explain the different efficiencies of signal transmission in alkaline and acidic zones is based on the so-called CO_2 hypothesis. The basic assumption is that the acidic regions are enriched with carbon dioxide. Therefore, local lighting causes abundant production and export of triose phosphates, which leads to large shifts in F' fluorescence at the terminal part of the signaling chain. In contrast, the alkaline zones are depleted of carbon dioxide, whereas bicarbonate and carbonate ions do not penetrate into the cell because of their charge. The lack of a substrate for the Calvin–Benson cycle would explain the low production and export of triose phosphates.

To assess this possibility, we measured the transient changes in chlorophyll fluorescence in response to local illumination in areas with different external pH values. The amplitude of fluorescence changes as a function of pH in cell surface layers had a sigmoid shape with a p$K \approx 9.3$, while the pK for equilibrium CO_2/HCO_3^- is 6.3 [43]. This result clearly deviates from the CO_2 hypothesis. Apparently, the local CO_2 concentration is not of primary importance for signal transmission, unlike the cytoplasmic pH, which affects the envelope translocators and stromal enzymes. The transmembrane proton flux is associated with opposite pH shifts on different sides of the membrane. One well-known example is that the photoinduced H^+ flux across the thylakoid membrane causes opposite pH shifts in the thylakoid and stroma: it lowers the lumen pH and elevates the stromal pH. The opposite pH shifts are also generated on different sides of bilayer lipid membranes during the induced proton transport in the presence of ionophores or weak bases [44]. By analogy, H^+ transport from the cytoplasm to the outer solution across the plasma membrane not only acidifies the medium, but also increases the cytoplasmic pH. Conversely, the H^+ influx induces the alkaline pH shift on the outer cell surface and should acidify the cytoplasm. Exactly this relationship between the transmembrane H^+ fluxes and cytoplasmic pH was revealed in growing pollen tubes of lily [45]. In the area of ATP-dependent proton efflux slightly away from the growing tip the cytoplasmic pH was almost 1 unit higher than in the region of passive H^+ influx (at the apex). It can be assumed that a similar pattern is observed in the case of characean algae.

Several treatments can be employed to test the assumed relationship between the lowered cytoplasmic pH under external alkaline zones and strong inhibition of cyclosis-mediated signal transmission. One of them consists in plasma membrane excitation: the generation of an action potential causes a prolonged cessation of H^+ influx and greatly attenuates the alkaline zones [46–49]. The high surface pH decreases sharply after cell excitation, and arrest of the inward H^+ flow should cause an alkaline shift of cytoplasmic pH. In these conditions, the amplitude of fluorescence changes caused by illumination of a remote cell area increased by five- to sixfold [43]. The second treatment exploits the ability of NH_4^+ to suppress the inward H^+ flow in the region of alkaline zones. Ammonium ions elevate the cytoplasmic pH because they permeate through the plasma membrane as neutral ammonia molecules and then bind protons in the cytosol. The pK value for NH_3/NH_4^+ equilibrium is 9.25. High pH in the alkaline zones determines the increased content of the neutral deprotonated form (NH_3), which facilitates the rapid permeation of this form into the cytosol. On the outer membrane side, the pH is shifted in the acidic direction. The fluorescence responses to local illumination recorded in the initially alkaline zone increased after adding NH_4^+ approximately tenfold, showing a similarity to the effect of the action potential [43]. This confirms the hypothesis that the cytoplasm beneath the alkaline zones of illuminated cells is slightly acidified under physiological conditions. Then, the long-distance interchloroplast communication is disrupted under external alkaline zones because of the lowered cytoplasmic pH in those cell regions where massive proton influx takes place.

As a further test of the CO_2 hypothesis, we attempted to determine whether the pH in the locally illuminated cell area is actually an important factor. If the longitudinal profile of external pH is experimentally determined, it is possible to arrange the optic fiber and the measurement region at the points with known pH values. Four measurement configurations were chosen and conventionally named according to the direction of fluid flow: (1) within the acidic zone, (2) from the acidic to alkaline zone, (3) within the alkaline zone, and (4) from the alkaline to acidic zone [26]. Assuming that the CO_2 sufficiency in external acidic zones is the critical factor that facilitates the

production of triose phosphates, one may expect that F' changes of equally large amplitudes would occur in configurations (1) and (2). However, the results were qualitatively different. It turned out that directing local light to the alkaline or acidic cell regions made no difference, whereas the outer pH in the analyzed area was quite important. In configurations 1 and 4, the changes in F' were large and approximately equal. In contrast, the F' changes were weak in configurations 2 and 3. Hence, different amplitudes of F' responses to bright local light cannot be assigned to abundant assimilate production in the acidic zones. A more likely cause is that the cytoplasmic pH differs under the alkaline and acidic zones, which affects the enzyme activities involved in transmission and transduction of metabolic signal. Thus, the terminal steps of the signal transmission chain, unlike its initial stages, display the increased sensitivity to alkaline pH on cell surface [26]. A certain role in different sensitivity of the proximal and distal segments of the signaling chain may belong to unequal light conditions, i.e., intense light pulses in the zone of metabolite export versus continuous dim light in the area of metabolite import and processing.

The presented method provides a means to investigate the transcellular movement of metabolites in cell chains [50]. Neighboring plant cells are interconnected by plasmodesmata, that is, plasmatic strands that penetrate the cell walls. Plasmodesmata contain individual actin filaments, but its content is apparently insufficient to maintain the transverse flow of the cytoplasm. The main proposed mechanism for the passage of assimilates through plasmodesmata is their diffusion. The plasmodesmal conductivity is assumed to be finely regulated. The supposed regulatory factors include the internal hydrostatic pressure and the cytoplasmic Ca^{2+} level. The conventional approach to studying the conductivity of plasmodesmata is based on the injection of fluorescein or its analogues into the cell and on subsequent detection of the delivery of the probe into neighboring cells [5, 6]. Compared to this method, chlorophyll fluorescence measurements have several advantages. The indicator is a native fluorescent probe, chlorophyll. The transported metabolites are formed in physiological quantities and only in the cytoplasm. No cell damage arises in the absence of microinjection. This method allows researchers to directly compare metabolite transport along the intracellular and transcellular pathways.

In the two experimental configurations that were used, the light source and the analyzed region were separated by an equal distance, but in one case the proximal and distal sections of the signal chain were located within the same cell, and in the other case they were placed in different internodal cells [50]. Figure 3 shows the changes in F' fluorescence observed during intracellular and transcellular passage of metabolites (curves *1* and *2*, respectively). Judging by the area under the curves, nearly 30% of the photometabolites carried along the donor cell eventually enter the adjoining cell. This percentage is surprisingly high, considering that the cytoplasmic flow in the vicinity of internode junction is directed tangentially to the cell wall and that the total cross-sectional area of plasmodesmata is less than 1% of the total intercellular surface. The time for passing the intercellular barrier was approximately 11 s and it did not depend on the distance between the local light source and the measurement zone [50]. The plots for the time of reaching the F' peak at various separating distance d were represented by parallel straight lines both for intracellular and the transcellular configurations. The time shift between these plots corresponds to overcoming the transcellular barrier, i.e., a single layer of nodal cells. Based on the measured time of metabolite passage from cell to cell and the known frequency of plasmodesmata in the porous cell wall, we estimated the diffusion coefficient of metabolites inside the plasmodesmata. According to our estimates, it was 3.6×10^{-8} cm^2/s, which is in close agreement with the data obtained by microinjection of fluorophores in another material (staminal hairs of *Setcreasea purpurea*) [6].

The transcellular passage of metabolites was found to be very sensitive to changes in the osmotic pressure of the medium. The replacement of the standard medium with a solution containing 0.15–0.2 M sorbitol completely suppressed the transcellular movement without affecting the intracellular transport. It should be noted that the osmotic treatment affected neither the velocity of cytoplasmic streaming nor the photosynthetic activity of chloroplasts. The block of plasmodesmal conductance imposed by elevation of external osmotic pressure (upon lowering the internal hydrostatic pressure) was completely removed when the cell was washed with a fresh medium. Thus, it is necessary to reconsider the accepted idea that the plasmodesmal conductance increases upon lowering the intracellular pressure [5, 51]. At variance with this idea, the results obtained on intact cells indicate the suppression of plasmodesmal conductance under osmotic and salt stress [50].

Thus, a new noninvasive approach to the study of long-range intracellular and intercellular transport has already provided diverse information on the role of cyclosis in the transmission of metabolic signals and on the properties of plasmodesmata. Forthcoming studies must elucidate the extent to which the chloroplasts that reside at the intermediate segment of the signaling pathway can consume and release metabolites during light–dark transitions. The microfluidic regulation of photosynthesis, of membrane ion fluxes, non-stationary dynamic structures, and plasmodesmal conductance under normal and pathological conditions are important issues in the area of cell biophysics and deserve further study.

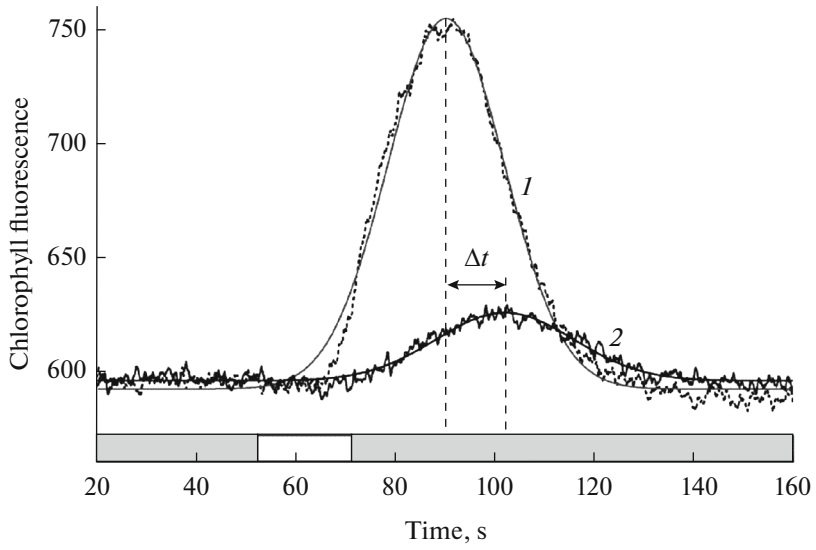

Fig. 3. The changes in *F'* chlorophyll fluorescence caused by the long-distance transmission of photometabolites within one internodal cell (curve *1*) and by their transcellular passage between adjacent internodes (curve *2*). The distance between the local illumination zone and the fluorescence measurement region in the intracellular and transcellular configurations was identical in both measuring configurations ($d = 1$ mm).

FUNDING

This study was supported by the Russian Foundation for Basic Research (projects nos. 16-04-00318 and 20-54-12015).

COMPLIANCE WITH ETHICAL STANDARDS

This article does not contain any studies with human participants or animals performed by any of the authors.

Conflict of Interest. The authors declare that they have no conflicts of interest.

REFERENCES

1. M. Tominaga and K. Ito, Curr. Opin. Plant Biol. **27**, 104 (2015).
2. T. Shimmen, J. Plant Res. **120**, 31 (2007).
3. R. E. Goldstein and J.-W. van de Meent, Interface Focus **5**, 20150030 (2015).
4. W. F. Pickard, Plant, Cell Environ. **26**, 1 (2003).
5. K. J. Oparka and D. A. M. Prior, Plant J. **2** (5), 741 (1992).
6. E. B. Tucker and J. E. Tucker, Protoplasma **174**, 36 (1993).
7. T. Nishiyama et al., Cell **174**, 448 (2018).
8. V. Z. Lunevsky, O. M. Zherelova, I. Ya. Vostrikov, et al., J. Membr. Biol. **72** (1), 43 (1983).
9. G. N. Berestovsky and A. A. Kataev, Eur. Biophys. J. **34**, 973 (2005).
10. W. J. Lucas and R. Nuccitelli, Planta **150**, 120 (1980).
11. M. J. Beilby, T. Mimura, and T. Shimmen, Protoplasma **175**, 144 (1993).
12. A. A. Bulychev, A. A. Cherkashin, A. B. Rubin, et al., Bioelectrochemistry **53**, 225 (2001).
13. A. A. Bulychev, A. A. Polezhaev, S. V. Zykov, et al. J. Theor. Biol. **212**, 275 (2001).
14. N. A. Krupenina, A. A. Bulychev, M. R. G. Roelfsema, et al., Photochem. Photobiol. Sci. **7**, 681 (2008).
15. N. A. Krupenina, A. A. Bulychev, and U. Schreiber, Protoplasma **248**, 513 (2011).
16. N. S. Allen and R. D. Allen, Ann. Rev. Biophys. Bioeng. **7**, 497 (1978).
17. T. Shimmen and E. Yokota, Curr. Opin. Cell Biol. **16**, 68 (2004).
18. T. McConnaughey, Limnol. Oceanogr. **36**, 619 (1991).
19. D. Menzel, Protoplasma **144**, 73 (1988).
20. I. Foissner and G. O. Wasteneys, J. Microsc. **247** (1), 10 (2012).
21. M. J. Beilby, Front. Plant Sci. **7**, 1052 (2016).
22. N. Kamiya, *Protoplasmic Streaming* (Springer, Wien, 1959).
23. R. Scheibe, Plant Physiol. **96** (1), 1 (1991).
24. M. Taniguchi and H. Miyake, Curr. Opin. Plant Biol. **15**, 252 (2012).
25. A. A. Bulychev, A. V. Alova, and A. B. Rubin, Eur. Biophys. J. **42**, 441 (2013).
26. A. A. Bulychev and A. A. Rybina, Protoplasma **255** (6), 1621 (2018).
27. A. V. Komarova, V. S. Sukhov, and A. A. Bulychev, Funct. Plant Biol. **45** (1–2), 236 (2018).
28. A. A. Bulychev and S. O. Dodonova, Russ. J. Plant Physiol. **58** (2), 233 (2011).
29. A. A. Bulychev and S. O. Dodonova, Biochim. Biophys. Acta **1807**, 1221 (2011).
30. A. A. Bulychev and A. V. Komarova, Protoplasma **251** (6), 1481 (2014).

31. A. A. Bulychev, in *Plant Electrophysiology: Methods and Cell Electrophysiology*, Ed. by A. G. Volkov (Springer, Berlin, 2012), pp. 273–300.
32. A. A. Bulychev and A. V. Komarova, Biochemistry (Moscow) **79** (3), 273 (2014).
33. A. A. Bulychev, *Long-distance Interactions and Signal Transmission in Chara Algae Cells: Timiryazev Memorial Lectures–76* (Nauka, Moscow, 2017) [in Russian].
34. S. O. Dodonova and A. A. Bulychev, Protoplasma **248**, 737 (2011).
35. A. A. Bulychev and A. V. Komarova, Biochim. Biophys. Acta **1847**, 379 (2015).
36. I. Foissner and G. O. Wasteneys, Plant Cell Physiol. **48** (4), 585 (2007).
37. A. A. Bulychev and I. Foissner, Plant Signal. Behav. **12** (9), e1362518 (2017).
38. A. A. Bulychev and A. V. Komarova, Protoplasma **254** (1), 557 (2017).
39. A. A. Bulychev, A. A. Rybina, and I. Foissner, in *Chloroplasts and Cytoplasm: Structure and Functions*, Ed. by C. Dejesus and L. Trask (Nova Science, New York, 2018), pp. 1–24.
40. A. A. Bulychev and N. A. Krupenina, Biochemistry (Moscow) Suppl. Ser. A: Membr. Cell Biol. **2** (4), 387 (2008).
41. C. H. Foyer and G. Noctor, Antioxid. Redox Signal. **11** (4), 861 (2009).
42. 42. A. A. Bulychev and A. V. Komarova, Biochim. Biophys. Acta **1858** (5), 386 (2017).
43. A. A. Bulychev and N. A. Krupenina, Bioelectrochemistry **129**, 62 (2019).
44. Y. N. Antonenko and A. A. Bulychev, Biochim. Biophys. Acta **1070**, 279 (1991).
45. J. A. Feijo, J. Saihas, J. R. Hackett, et al. J. Cell Biol. **144** (3), 483 (1999).
46. A. A. Bulychev and N. A. Kamzolkina, Bioelectrochemistry **69**, 209 (2006).
47. A. A. Bulychev, N. A. Kamzolkina, J. Luengviriya, et al., J. Membr. Biol. **202** (1), 11 (2004).
48. A. A. Bulychev and N. A. Krupenina, Plant Signal. Behav. **4** (8), 24 (2009).
49. N. A. Krupenina and A. A. Bulychev, Biochim. Biophys. Acta **1767**, 781 (2007).
50. A. A. Bulychev, Protoplasma **256** (3), 815 (2019).
51. V. Hernandez-Hernandez, M. Benitez, and A. Boudaoud, J. Exp. Bot. **71** (3), 768 (2020). https://doi.org/10.1093/jxb/erz434

Translated by A. Bulychev